Measuring and modeling per-element angular visibility in multiview displays

Atanas Boev, Robert Bregovic, Atanas Gotchev
Department of Signal Processing, Tampere University of Technology, Tampere, Finland
firstname.lastname@tut.fi

ABSTRACT

Multiview displays employ an optical layer, which distributes the light of an underlying TFT-LCD panel in different directions. Certain properties of the layer create specific artifacts, such as ghost images, moiré patterns and masking. We model the layer as an image processing channel and identify display parameters related with the model, which are important for design of image processing algorithms for artifact mitigation. The identified parameters are interleaving pattern, angular visibility and frequency throughput of the display. We present a methodology for deriving these parameters for an arbitrary LCD-based multiview display, which does not require precisely positioned measurement equipment. As a case study, we present measurement and modeling results for a particular multiview display.

1. INTRODUCTION

Multiview displays are a class of autostereoscopic displays, which can be used without the need of special glasses and can be watched by multiple users simultaneously [1, 2, 3, 4, 5, 6, 7]. Multiview displays generate multiple observations of a scene, each one seen from a different angle. Usually, the image is formed on a TFT-LCD. An additional directionally selective *optical layer* mounted on top of the LCD redirects the light of the sub-pixels in different directions [1, 4, 7, 18]. The layer is either a *parallax barrier*, which blocks the light in some directions[7] or *lenticular sheet*, which works by refracting the light[8]. The apparent brightness of each sub-pixel is a function of the angle. The group of sub-pixels which is visible from one direction forms an image, known as *view* [1, 7, 9]. From a certain spot in front of the display, all sub-pixels that belong to a view are seen with maximal brightness. Such a spot is referred to as an *optimal observation spot* for the corresponding view. Outside of that spot, there is a larger *view visibility zone*, in which the view is still visible, albeit with diminished brightness. In LCD-based multiview displays, views are spatially multiplexed [1,2,9]. The process of mapping multiple images to the views of one display is called *interdigitation*[9], *view multiplexing*[1], *interlacing*[3, 5] or *view interleaving*[14]. The latter term is adopted in this paper. The relation between the position of a sub-pixel and the view it belongs to is given by an *interleaving map*. Since both the LCD and the optical layer have a repetitive structure, the interleaving map can be described by a periodic *interleaving pattern* [7, 9]. The pattern is spatially independent – the angular visibility of a sub-pixel depends on its position in respect to the pattern, but not on its absolute position in respect to the display.

The design of a multiview display is a trade-off between observation convenience and visual quality. The added convenience in using multiview display comes at the expense of limited brightness, contrast and resolution [1,9,10]. The optical layer is a source of specific visual artifacts[1]. These are moiré patterns caused by aliasing [9, 11,13], ghost images caused by crosstalk [7,10, 19] and masking artifacts, caused by the optical layer behaving like an up-sampling block. The masking artifacts manifest themselves as a fine mesh superimposed over the image, an effect that can be regarded as imaging, as discussed in Section 5. The influence of these artifacts on the visual quality of a 3D scene depends both on image content and optical parameters of the display. It is possible to use image processing methods to mitigate these artifacts [5, 9, 13, 14], and the effectiveness of the image processing methods depends highly on the information about the optical characteristics of the display, which is, however, rarely available to the end user.

There are various methods for assessing the optical quality of the display – for example, using directional scanning for 2D [15] and 3D [10] displays. In [8] the authors propose an extensive list of optical parameters which can be measured for characterization of autostereoscopic 3D displays. In this paper, we aim to identify and measure the parameters that can be used for visual optimization. Thus, we are interested in the parameters that are important from the image processing point of view, rather than in ones which describe the optical quality of a 3D display.

The paper is organized as follows. In Section 2, we propose a model, which considers a multiview display as an image-processing channel. The model is used to describe the typical visual artifacts in signal processing terms. The parameters in this model identify which characteristics of the display are needed in visual optimization algorithms. In Section 3 and Section 4 we present a simple, yet effective, methodology to measure and model these parameters. More specifically, in

Section 3 we describe a way to derive the interleaving topology, and in Section 4 we propose a method for finding the angular visibility of each display element by combining measurement data from several points. Finally, in Section 5, we characterize the properties of the display in the frequency domain. As a case study, this paper presents measurement results for 23" 3D Display AD built by X3D-Technologies GmbH, which is hereafter referred to as *X3D display*.

2. MULTIVIEW DISPLAY AS IMAGE PROCESSING CHANNEL

Multiview 3D displays aim to generate multiple images, each one seen from a different observation angle. The optical layer mounted above the screen surface acts as directionally selective filter and applies angular luminance function to each sub-pixel of the display. The angle, at which the angular luminance has its peak value, determines the optimal observation direction of the sub-pixel. There are groups of sub-pixels with similar angular luminance functions, which are simultaneously visible, thus creating the illusion of an image which is visible from certain angles and invisible from others. The number of groups with a similar angular luminance function determines the number of views generated by the display.

The interleaving map can be represented as a set of non-overlapping lattices, where each lattice contains sub-pixels from a single view only [9]. On an image with the full resolution of the LCD, each of these lattices acts as a rectangular sub-sampling pattern with a different offset. An example is shown in Figure 1a, where the intersecting dotted lines mark the position of LCD sub-pixels; one lattice is marked with circles and another is marked with crosses. The horizontal step of the lattice is equal to the width of the interleaving pattern (denoted with n_{patt} in Figure 1a) and the vertical step equals to the height of the pattern (denoted with m_{opt} in the same figure). All the sub-pixels that appear on column $k * n_{patt}$ and row $k * m_{patt}$, where k is an integer, belong to a group with equal angular visibility. The sub-pixels that appear on column $k * n_{patt} + x$ (for $0 \le x < n$) and row $k * m_{patt} + y$ (for $0 \le y < m$) also belong to a group with equal angular visibility. It is possible that more than one of these groups belong to the same view.

A model of a multiview display as an image processing chain is shown in Figure 1b. We assume that as input we have v images with full resolution, which have to be mapped to v views generated by the display. Out of each image, only sub-pixels that belong to the corresponding view are used. This is modeled by a 2D downsampling operation. Since the views are spatially multiplexed, each image gets sampled with different offset, represented by image shift $z(x, y)$, where x, y are the horizontal and vertical offset. On the display, the sub-sampled image is represented in its original size. The visible sub-pixels appear either surrounded by black stripes by the parallax barrier or enlarged by the lenticular sheet. This effect is modeled as an upsampling stage, where the introduced samples are either set to zero, or are a repetition of the same sample value. Since several groups of p sub-pixels can belong to the same view, downsampling and upsampling in the most general cases, is not performed on a rectangular grid.

The angular luminance is modeled as a function of the observation angle. We model the effect of the optical layer on the brightness of underlying pixels as *visibility* – the ratio between the relative brightness of a view and the maximum brightness of the display as seen from the same angle. The function $f(\theta + k_v)$ gives the visibility of view v from observation angle θ. We refer to such function as *horizontal angular visibility*. We assume that the function is the same for all views, with the peak visibility of each view occurring at different observation angle. With k_v we denote the offset of the function for view v.

Using the proposed model, typical visual artifacts on multiview displays can be explained from the signal processing point of view. Aliasing occurs if the source images have not been suitably pre-filtered with an anti-aliasing filter before downsampling. The design of an anti-aliasing filter relies on knowledge of the interleaving topology [9, 13, 14]. The topology can be derived by finding n, m and all combinations of x and y that belong to the same view. Ghost images occur when images with different offset are simultaneously visible – this effect can also be regarded as crosstalk. Crosstalk mitigation algorithms need knowledge of the angular visibility function [13,19], which is denoted as $f(\theta + k_v)$ in our model. Due to the optical layer, the visible parts of sub-pixels have a non-rectangular shape [16, 17, 18] and the gaps between them are directionally oriented. The presence of gaps creates effects similar to the ones caused by upsampling in the absence of a post-filter. In sampling and interpolation literature the effect is denoted as 'imaging' and the filters tackling it are known as anti-imaging filters. In the case of multiview displays, this effect is best quantified by analyzing the performance of the display in the frequency domain.

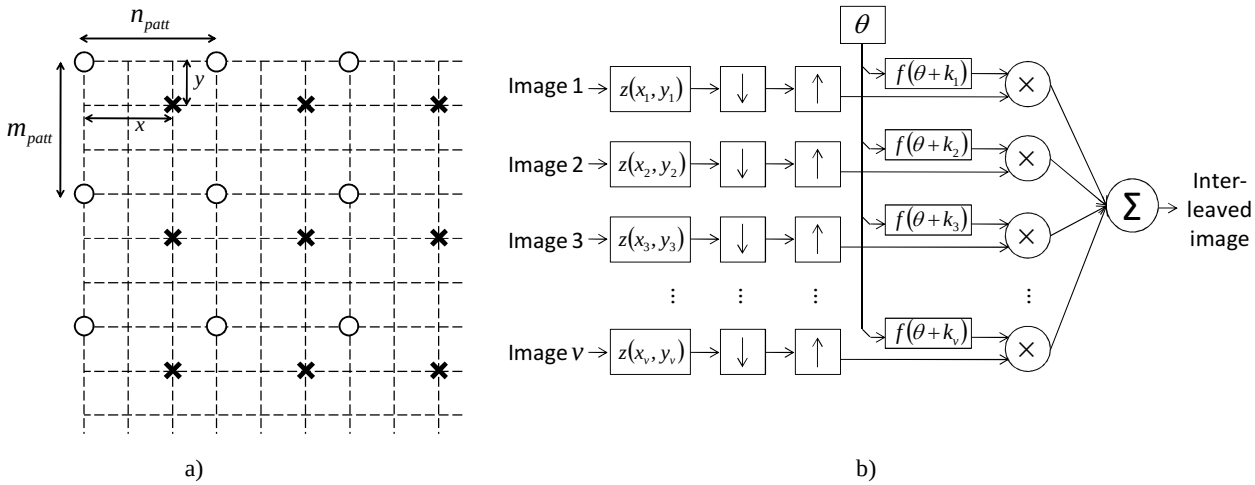

Figure 1. Model of the optical layer effect as an image processing channel: a) interleaving map as a set of non-overlapping lattices and b) interleaved image as a weighted sum of sampled images

3. DERIVING THE INTERLEAVING PATTERN

In some cases, the description of the interleaving pattern is partially or fully missing in the documentation provided along with the display. This prompts proposing a methodology for deriving the pattern. Our proposed methodology has four steps – finding the minimal width and height of the pattern (n_{patt} and m_{patt} in Figure 1), obtaining the number of views generated by the display, and finally, deriving the complete interleaving pattern.

Ideally, a view should be visible with maximum brightness from a limited range of observation angles and be invisible from anywhere else. An example of angular visibility of a view is given in Figure 2a, with "visible" and "invisible" regions marked with "V" and "N", respectively. We refer to the ratio between the width of "N" and "V" regions as *visibility separation*. A group of sub-pixels with similar angular visibility has a higher overall N/V ratio than a group where each sub-pixel has a different optimal observation point. The "optimal" interleaving pattern of a 3D display is one that separates the sub-pixels into groups that yield the highest visibility separation.

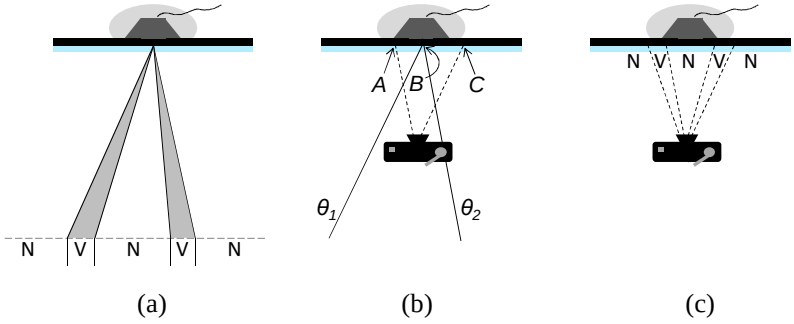

Figure 2. Angular visibility of multiview display: a) visibility separation, b) observation angles when taking a close shot, and c) close observation of angular visibility

In order to study the angular visibility of a sub-pixel one can selectively activate groups of sub-pixels and perform an angular scan [5], or use Fourier optics to study a point on the screen from many angles simultaneously[20]. Our approach is to observe the display from a distance shorter than the optimal one, utilizing the space-invariance of the pattern. In this approach, the visibility of multiple sub-pixels as seen in one camera position is related to the visibility of one sub-pixel as seen from multiple camera positions. As exemplified in Figure 2b, point "A" observed from close distance is seen from the same angle as point B observed from the optimal observation distance at angle θ_2. Similarly, point "C" as seen from a closely positioned camera should have the same visibility as point "B" from observation angle θ_2. We refer to images taken from a closely positioned camera as *close shot* images. In the close shot, a horizontal line of the screen is expected to have visibility proportional to the horizontal angular visibility of a point from the optimal observation angle, as seen in Figure 2c. The higher the angular visibility ratio (as seen in Figure 2a) is, the higher is the N/V ratio of the horizontal line (as seen in Figure 2c). In our experiments, the distance between display and camera was 8cm.

3.1 Finding pattern width

The optimal width of the interleaving pattern is found by observing a row of sub-pixels, probing for different pattern widths, and selecting the set with the highest visibility separation.

First, one should take a close shot of a square with known size in sub-pixels and use it to estimate the camera orientation and to determine the ratio k between display pixels and pixels in the acquired photograph. This allows estimating where each photographed sub-pixel appears on the photo, regardless of the exact camera placement. The next step is to activate every n-th sub-pixel in one row (as seen in Figure 3a), and take a close shot. As the line consists of discrete sub-pixels, the angular visibility of the view would appear sampled at discrete angles. In order to evaluate the visibility separation, one should distinguish dark pixels in "N" regions masked by the optical layer, and dark gaps in "V" regions caused by inactive sub-pixels. The width of the gaps in the "V" zones is proportional to the currently probed pattern width n. To make the distinction, we apply a maximum value filter in a horizontal direction using window size of $n * k / 3$ (k is divided by 3 to obtain the display ratio per sub-pixel).

By probing for various values of n, one can obtain the visibility separation for interleaving pattern with the corresponding widths. The maximum n is bounded by the expected number of views: we used $1 < n < 64$ in our experiments. A test image containing lines with different n can be seen in Figure 3a. The same image, as seen on a close shot of the X3D display, is in Figure 3b. The processed image, where each line is filtered with the corresponding maximum value filter, is shown in Figure 3c. By counting consecutive black pixels in each row, one can find the minimal n which has the highest visibility separation. In our experiments this is $n_{patt} = 8$.

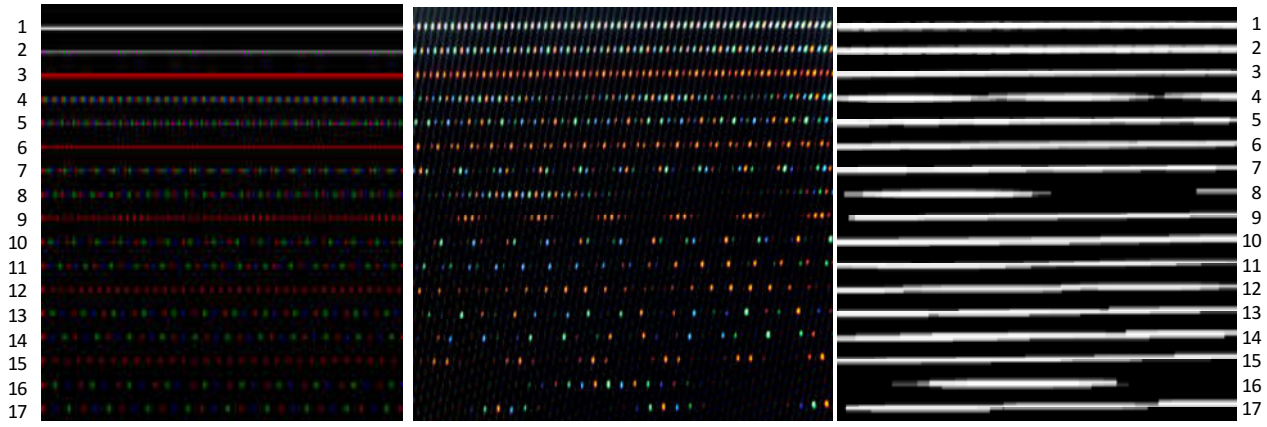

(a) (b) (c)

Figure 3. Deriving the width of interleaving patten: a) test image containing lines with different step size b) close observation of the test image, b) test image, processed with maximum value filter with coressponding window size.

3.2 Finding pattern height

The minimal height m_{patt} of the interleaving pattern can be found by testing patterns with optimal width and variable height m. The test image for pattern $n \times m$ has sub-pixels on every n-th sub-pixel column and every m-th pixel row lit. Each row in that image has optimal visibility separation, but if the optical layer is mounted at a slant, the position of the "V" zones might differ across the rows. For some values of m, the optimal observation directions for each row coincide, making all active sub-pixels simultaneously visible from certain observation directions. If one considers the mean brightness of all visible sub-pixels, the optimal m is the value which yields the highest visibility separation for the display as a whole.

Unfortunately, from a close position the angle from which the display rows are seen varies in the vertical direction as well. Thus, from a single close shot it is impossible to predict whether the optimal observation points of each row would coincide at some distance. However, most multiview displays aim to provide views which spread in the horizontal direction only[1,7, 18]. In that case, the angular visibility of the display should change frequently in the horizontal and less often in the vertical direction. In the close shot, this corresponds to vertical lines with minimal slant. In order to distinguish non-visible from inactive sub-pixels, one can apply a two-dimensional maximum value filter with window size of $(n * k / 3) \times (m * k)$, where n, m are the size of the pattern used in each test. The filtered image with lowest frequency in the vertical direction corresponds to the optimal size of the interleaving pattern.

The top row of Figure 4 shows close shots of different test patterns on X3D display, and the bottom row shows the corresponding processed images. In our measurements, we used the position of the biggest peak in the 2D frequency response to determine the slant of the lines, and found pattern size of 8×12 to be the optimal one.

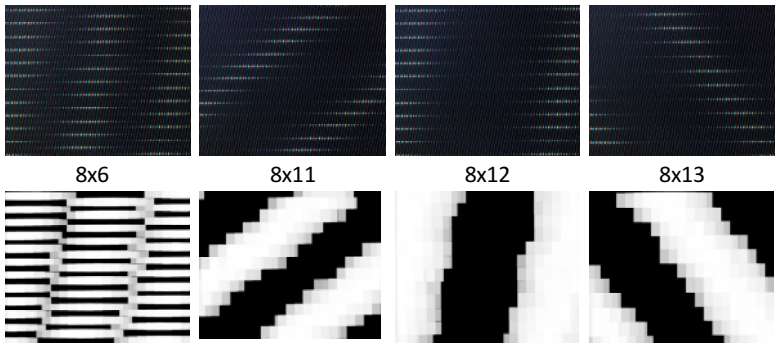

Figure 4. Deriving the height of the interleaving pattern: top row – close observations of test patterns with various heigths; bottom row – the same, processed with maximum value filter with corresponding window size.

3.3 Number of views

It is possible that a display with interleaving pattern of $n_{patt} \times m_{patt}$ generates less than $n_{patt} \cdot m_{patt}$ views, i.e. there are sub-pixels with different coordinates in the pattern which belong to the same view. This case can be tested by building a test image using the optimal pattern size with only one sub-pixel in the pattern lit, as shown in Figure 5a. We refer to these images as *test pattern*, followed by the row and column where the active sub-pixel is positioned. For example, test pattern "R4C7" is a test image that consists of a periodic pattern with size $n_{patt} \times m_{patt}$, where sub-pixel on row 4, column 7 is lit. The total number of such test pattern images is $n \cdot m$. If two test patterns contain pixels that belong to the same view, they would have identical angular visibility and contribute light to the same regions in the close shot.

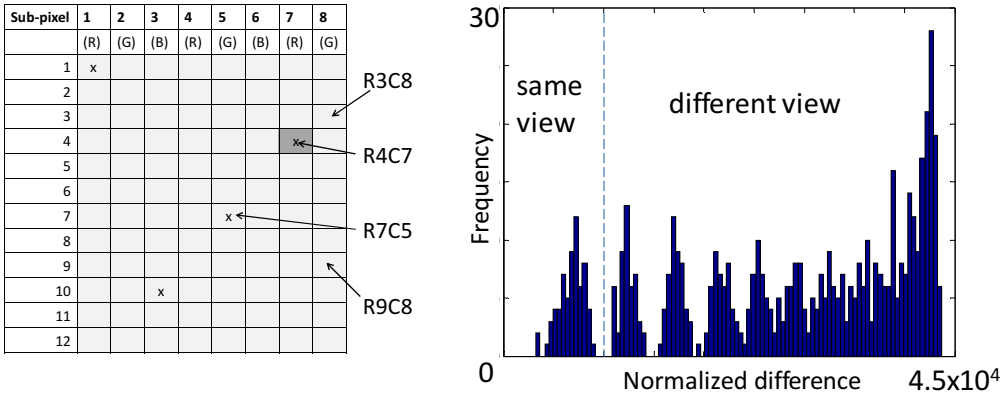

(a) (b)

Figure 5. Single-sub-pixel test patterns: a) position of sub-pixel in the pattern (pixels marked with "x" are found to belong to the same view), b) normalized differences between close observations of all test patterns

The close shots need to be processed with a max value filter with window size of $(n_{patt} * k/3) \times (m_{patt} * k)$ as is done in the previous section. Test patterns with sub-pixels which belong to one view should produce slightly different output, since sub-pixels of those patterns appear on different coordinates of the display. However, test patterns with different angular visibility should produce noticeably different results. The norm of difference between two output images can be used to determine if two test patterns belong to the same view or not. One can calculate the l^2-norm of the difference between each pair of filtered images, build a histogram of all norms, and find the threshold between "similar" and "different" norms, as shown in Figure 5b. The first group in the histogram represents differences between "similar" patterns that belong to the same view.

Close shots of X3D display exhibiting some test patterns and their filtered counterparts are given in Figure 6. In this example, sub-pixels "R4C7" and "R7C5" were found to belong to the same view. Test patterns with normalized difference lower than the threshold were grouped together. The whole set of 96 test patterns produced 24 distinctive

groups of 4 patterns each, which means that X3D display is able to generate 24 distinctive views. Sub-pixels, which belong to the same group, are marked with "x" in Figure 5a.

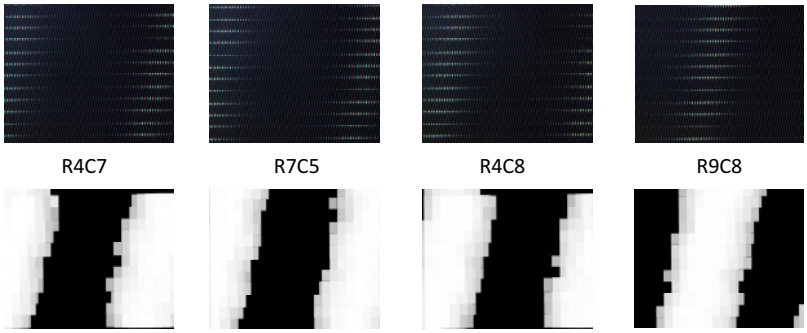

Figure 6. Deriving number of views: top row – close observations of various test patterns; bottom row – the same test patterns after filtering. Sub-pixels which belong to the same view produce similar close observations (the similarity threshold is shown in Fig. 5b)

3.4 Interleaving topology

The final step is to assign a view number to each group of sub-pixels with similar angular visibility. The order of the views is arbitrary, but for practical reasons it is preferred that views with neighboring observation zones have consecutive numbers. To enumerate the views in that order, one should find the visibility zone of each view.

A set of $v_{\max}$ test images is prepared, where $v_{\max}$ is the derived number of views. In each test image, all sub-pixels belonging to the same view are lit. We refer to these images as *single-view* ones. By observing a single-view image on the display, one can search for an observation position from which the display is seen with maximal mean brightness. This position is the optimal observation spot of the corresponding view.

In our experiments we could identify visibility zones with fuzzy borders, appearing approximately on a line, in front of the display, as shown in Figure 7a. As this result is consistent with the measurements of other displays [5,20], we approximated optimal observation spots to be equidistant on the line, as marked with "X" in Figure 7a. In our measurements, the distance between the display and the line was approximately 140cm.

In our experiments, we enumerate the zones from left to right, so that middle zone numbers are aligned with the center of the display. By labeling the sub-pixels with corresponding numbers, we obtain the interleaving pattern for X3D display as shown in Figure 7b.

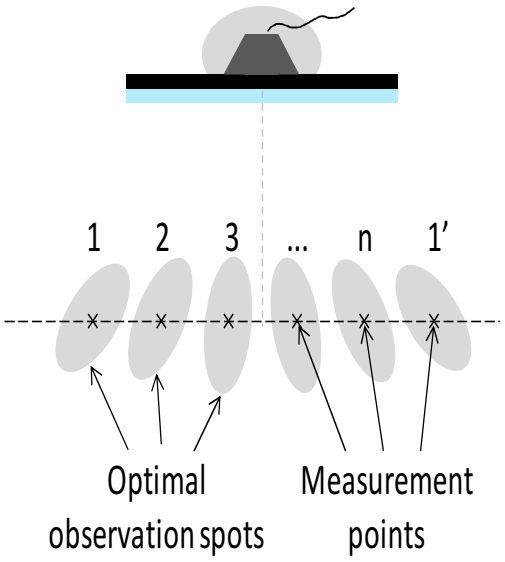

(a)

Pixel column 1 Pixel column 2 Sub-pixels columns

Pixel rows	1 (R)	2 (G)	3 (B)	4 (R)	5 (G)	6 (B)	7 (R)	8 (G)	9	10	11	12
1	2	5	8	11	14	17	20	23	2	5	8	11
2	4	7	10	13	16	19	22	1	4	7	10	13
3	6	9	12	15	18	21	24	3	6	9	12	15
4	8	11	14	17	20	23	2	5	8	11	14	17
5	10	13	16	19	22	1	4	7	10	13	16	19
6	12	15	18	21	24	3	6	9	12	15	18	21
7	14	17	20	23	2	5	8	11	14	17	20	23
8	16	19	22	1	4	7	10	13	16	19	22	1
9	18	21	24	3	6	9	12	15	18	21	24	3
10	20	23	2	5	8	11	14	17	20	23	2	5
11	22	1	4	7	10	13	16	19	22	1	4	7
12	24	3	6	9	12	15	18	21	24	3	6	9
13	2	5	8	11	14	17	20	23	2	5	8	11
14	4	7	10	13	16	19	22	1	4	7	10	13
15	6	9	12	15	18	21	24	3	6	9	12	15

(b)

Figure 7. Deriving the interleaving topology: a) measurement points in the approximate centers of the optimal observation spots (view from the top); b) interleaving pattern for X3D display

4. ANGULAR VISIBILITY OF EACH SUB-PIXEL

In general, doing an angular scan to obtain the visibility as a function of the angle requires precise positioning – otherwise the angular visibility curve is sampled at irregular intervals. In our method, we measure the visibility of each view at arbitrary points along the optimal observation distance, and search for single function that gives the best fit for all measurements regardless of the observation point.

4.1 Measurements

As a first step, one needs to prepare all the single-view images that correspond to the views generated by the display. Then the measurement points have to be selected as close as possible to the centers of the visibility zones. In our experiments, twenty-five measurement points were selected. Twenty-four of them are in the visibility zones of each view, and the last one is in the visibility zone of the first replica of view 1, as marked with "X" in Figure 7a. Observation point 13 appears in the center.

The next step is camera calibration. Camera sensitivity and aperture should be set to a minimum to minimize CCD noise. Camera exposition should be chosen such that the maximum pixel value in the shots is under the range in which camera response gets into saturation. Then the camera response function should be linearized in the fashion described in [22]. In our experiments, we used 16 gray-level test images where all pixels were set to values between 0 and 255, with step of 16. All the test images were shot in a dark room from measurement point 13.

The last step is measuring the angular visibility. One should prepare $v_{\max}$ single-view images, where $v_{\max}$ is the number of views generated by the display. Additionally, one *white image* with all sub-pixels set to maximum brightness and one *black image* with all sub-pixels set to zero are needed. From each observation position the white, black and all single-view images should be photographed. The set of images shot from one point is rectified using the corners of the display in the white image. For each single-view image, the mean brightness in the center of the display is measured, and normalized to range from zero to one, where zero is the mean brightness measured for the black test image, and one is the brightness measured for the white test image.

In our measurements, from each measurement point we took 26 shots of X3D display, showing the black, white and 24 single-view test images. After normalization we obtained 25 sets of 24 measurements indicating the brightness of each view relative to the full brightness of the display for each observation position. Because of the normalization, the maximum measured brightness is approximately the same (close to 0.5) for all angles. We used the normalized measurement as visibility $S_p(v)$, where v is the view number and p is the measurement point. The results for four measurement positions are shown in Figure 8.

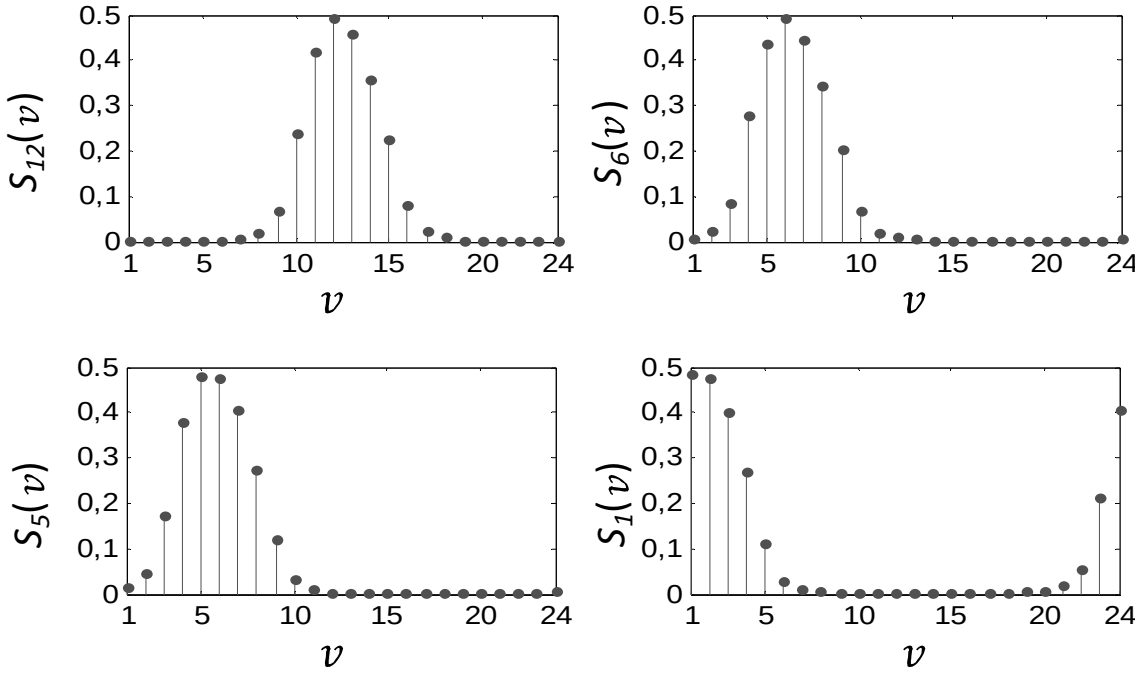

Figure 8. Measurement results for X3D display for measurement points 12 (top-left), 6 (top-right), 5 (bottom-left) and 1 (bottom-right).

4.2 Modeling angular visibility

If the measurement point is displaced from the center of a visibility zone, the visibility function gets sampled with an offset, and the maximum value of that function falls in between two samples. However, judging by the measurement results in other work [7, 20] we assume that the visibility curve for all observation points can be closely approximated by the same function, which has its peak occurring in the optimal observation spot for the corresponding view. We use τ_p to denote the offset of the visibility curve. Integer values of the offset τ_p correspond to the angular visibility in an optimal visibility spot, and non-integer values of τ_p correspond to the angular visibility between spots. Based on this assumption, one can search for a single function that closely fits measurements for all positions regardless of possible offset τ_p. We decided to fit a periodized Gaussian function,

$$G_{a,\sigma,\tau}(v) = \sum_{k=-\infty}^{+\infty} a e^{-\frac{(v-\tau-kv_{\max})^2}{2\sigma^2}}, \tag{1}$$

where $v = 1,\ldots,v_{\max}$ and search for optimal (a,σ) that will give the minimum fit error in:

$$\arg\min_{a,\sigma\in\mathrm{R}^+}\left(\sum_{p=1}^{p_{\max}} \arg\min_{\tau_p\in\mathrm{R}} \left\| G_{a,\sigma,\tau_p} - S_p \right\|_2^2\right) \tag{2}$$

where $p_{\max}$ is the total number of measurement points and $v_{\max}$ is the total number of views.

The resulting Gaussian function for X3D-display with $a = 0.51, \sigma = 7.49$ is shown in Figure 9a, along with $S_{12}(v)$. By sampling this curve for integer values of v and $\tau_p = v$, one can get the visibility of each view for observation point p. By replacing the view numbers in the interleaving map with their visibilities, one can obtain the visibility of each sub-pixel for observation point p.

Since the visibility curve is the same for all observation positions, and the optimal observation points are equispaced, we can assume that the visibility of one view from different observation points follows the same function as visibility or different views from one observation point. In that case one can estimate the visibility between two optimal observation positions by choosing fractional τ_p. As an example, $G(v)$ for $\tau_p = 5.5$ is shown in Figure 9 along with actual measurements done from an observation point that lies between points 5 and 6.

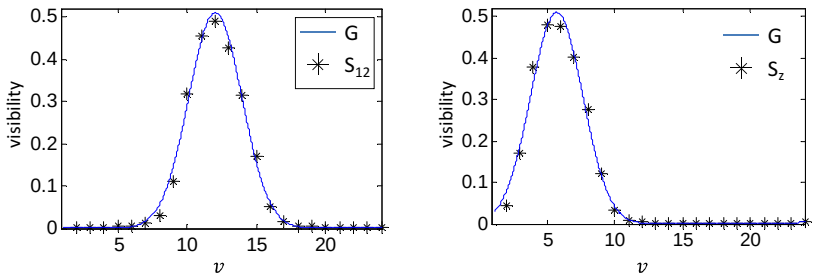

(a) (b)

Figure 9. Modeling angular visibility: a) shape of derived Gaussian curve (G) with measurements for observation point 12 (S12), b) predicted visibility of all elements (G) between observation points 5 and 6, with measurements done in that point (Sz).

5. PERFORMANCE ANALYSIS OF A MULTIVIEW DISPLAY IN THE FREQUENCY DOMAIN

Based on the measurements described in the previous sections we can determine the visibility of every pixel on the LCD matrix from an arbitrary observation point. At the same time, due to the structure of the display, only a fraction of the pixels will be visible from one observation point (view). In addition, there are gaps between the visible sub-pixels in one view. Thus, when visualizing full-size images (i.e. images with resolution equal to the LCD matrix resolution) there are two effects involved: aliasing due to the picking up of sub-pixels on non-rectangular grid and imaging, due to the

presence of gaps- aliasing can be fully tackled by an anti-aliasing pre-filter. Usually, imaging is tackled by an anti-imaging post-filter. As the imaging is created by the physical structure of the display, it is impossible to impose a post-filter. However, the effect can be partially mitigated by a pre-filter. In order to determine the properties of the required 2D filter, and consequently have the best possible representation of images on the display (minimizing aliasing, imaging and ghosting), it is necessary to determine the performance of the display in the frequency domain; that is, we have to know which frequency components in the image we can keep (ones that will be properly represented on the screen), and which ones we have to attenuate (remove) as potential causes of distortions.

Determining the performance of the display in the frequency domain is challenging. Based on the interleaving pattern determined in Section 3 and the display model given in Figure 1b, one could derive an analytical expression of the frequency domain behavior of the display. However, this theoretical approach does not take into account several effects occurring on the display. First, the visible sub-pixels are not on a rectangular grid (See Section 3). Second, every visible sub-pixel is seen with a different intensity (See Section 4). Finally, due to the masking effects, the pixels have a non-rectangular shape [16, 17, 18]. The combination of these effects creates an intensity distribution map, which alters the brightness of each image element in a non-linear fashion. Assuming that we could somehow model all nonlinear effects, the analytical approach would become mathematically very demanding. Moreover, due to the fact that in the general case we do not know the exact properties of all parts of the screen (optical layer, slant of the barrier, thickness, etc.) in the theoretical approach many tradeoffs would have to be made, thereby ending with a frequency response that might or might not describe the display well enough. In order to achieve a practical solution, it turns out that for deriving the frequency response of the display it is much more convenient to use a measurement-based approach, as described in this section. In the derived frequency response we will denote as *passband* the region in the frequency domain containing frequencies that are properly represented on the screen. All other regions will be denoted as *stopband.*

The main idea in the proposed approach is to generate several images containing signals with various known frequencies, visualize them on the display, and then compare the output of the display with the input images. We illustrate the procedure for the X3D display, but the approach itself is perfectly applicable for any other multiview display.

5.1.1 Preparing test images

The first step in measuring the frequency response of the display is to generate appropriate test images. For this purpose we prepared several hundred images, each of them being a pattern of a fixed known frequency. Two of these images for frequencies $(f_x, f_y) = (0.1, 0.1)$ and $(f_x, f_y) = (0.2, -0.3)$ are shown in Figure 10 with the corresponding spectra shown as contour plots in Figure 11. Here, f_x and f_y refer to frequencies along the x and y axis, respectively. The frequencies are normalized to $f_s/2=1$, with f_s being the sampling frequency. We can see in Figure 11 that each of these signals has distinct peaks in the spectra (the peak at $(f_x, f_y) = (0, 0)$ is the DC component and should be ignored). The motivation for using such images lies in the fact that by knowing exactly what image we sent to the display, based on what we see on the display, we can determine the properties of the display in the frequency domain.

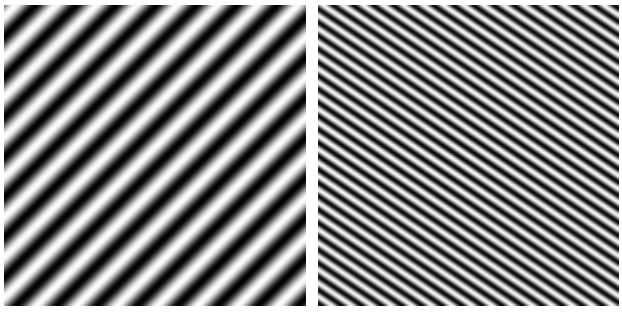

(a) (b)

Figure 10. Example of input (test) images: a) $(f_x, f_y) = (0.1, 0.1)$ and b) $(f_x, f_y) = (0.2, -0.3)$.

We assume no a priori knowledge about the display properties. Therefore, the test images must be generated for all sets of frequencies (f_x, f_y) with $f_x \in [0, 1]$ and $f_y \in [-1, 1]$. The signals for $f_x \in [-1, 0)$ and $f_y \in [-1, 1]$ can be easily reconstructed by taking into account the symmetry properties of the spectra of real signals. In order to obtain a precise frequency response of the display, we have to use a very dense grid of frequencies. However, a very dense grid means a high number of images which, in turn, will require a lot of measurements. Therefore, we suggest that first a larger grid is used, e.g. $\Delta_f \geq 0.1$, to roughly determine the properties of the screen and then repeat the measurement with a denser

grid, e.g. $\Delta_f \approx 0.1$, in the regions around the edges of the passband. In this paper, for the X3D display, we used the step $\Delta_f = 0.025$.

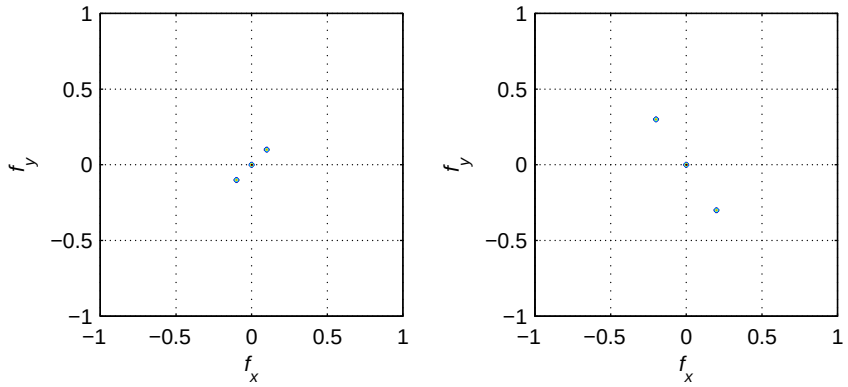

Figure 11. Example of input images – Spectra (contour): a) $(f_x, f_y) = (0.1, 0.1)$ and b) $(f_x, f_y) = (0.2, -0.3)$.

5.1.2 Measurements

The second step in measuring the frequency response of the display is to visualize the above described input images on the display and take photos of the screen by using a high resolution digital camera. The photos were taken from a distance of approximately 40cm from the screen. Although the distance is not critical, the camera should not be put too close to the screen in order to avoid interference between multiple views. The photos taken by the camera will be hereafter referred to as output images. As an example, for the input images shown in Figure 10, the output images are shown in Figure 12 (the images have been enhanced for clarity) with the corresponding spectra given as contour plots in Figure 13. Please note that due to the fact that k, the ratio between pixels on the display and pixels in the output images, is less than one, after evaluating the spectra, the frequencies have to be rescaled by the factor $1/k$. This scaling has been already included in Figure 13.

Several observations can be made based on these measurements. First, although each of the input images contains only a single frequency component, the output images contain many distinct frequency components. This is mainly due to the aliasing and imaging effects of the display. This is modeled in Figure 1 through down-sampling and up-sampling blocks.

Second, although there are many high frequency distortions in the output image due to imaging, which is in turn due to the physical gaps between visible sub-pixels, those imaging components are partially suppressed by the human visual system. Therefore, we are still able to see properly the input signal on the display as long as the input signal contains only sufficiently low frequency components. This is illustrated in Figure 12a and Figure 12b. In the first figure, the diagonal lines are still seen even if they are heavily broken, but in the second figure, beside the barely visible diagonal lines from Figure 10b, many other lines are also seen and therefore we cannot properly identify the input signal. Imaging is an issue as it occurs at the display and we do not have any possibility to remove it.

Third, the display introduces non-linear distortions, as illustrated in Figure 14. This figure shows the spectra along the x-axis for the input signal $(f_x, f_y) = (0.2, 0)$ and the corresponding output signal. Although the input signal has only one spectral component at $f_x = \pm 0.2$, the output signal also contains harmonics at $f_x = \pm 0.4$ that are approximately 6-8 dB lower than the main spectral component.

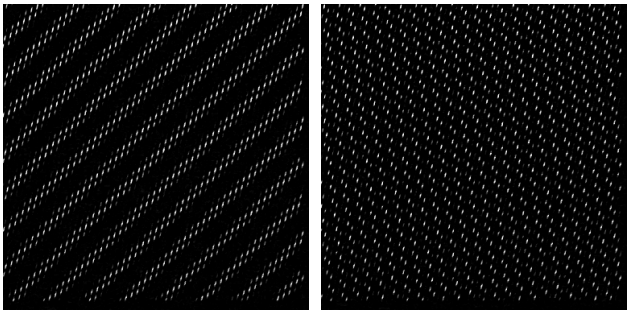

Figure 12. Example of output images (photos taken from the display): a) $(f_x, f_y) = (0.1, 0.1)$ and b) $(f_x, f_y) = (0.2, -0.3)$.

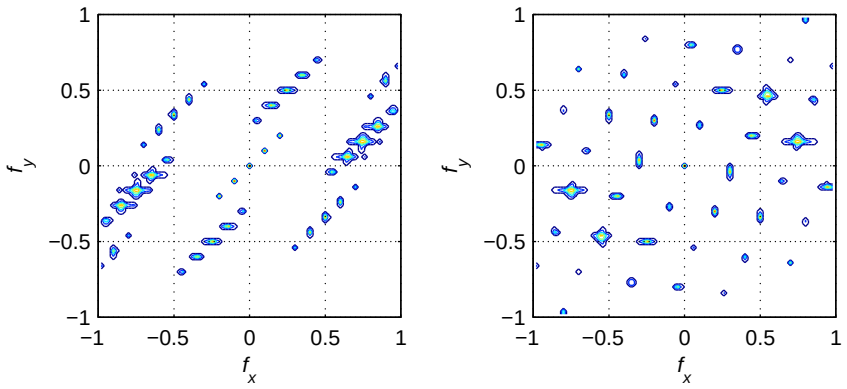

(a) (b)

Figure 13. Example of output images – Spectra (contour): a) (f_x, f_y) = (0.1, 0.1) and b) (f_x, f_y) = (0.2, –0.3).

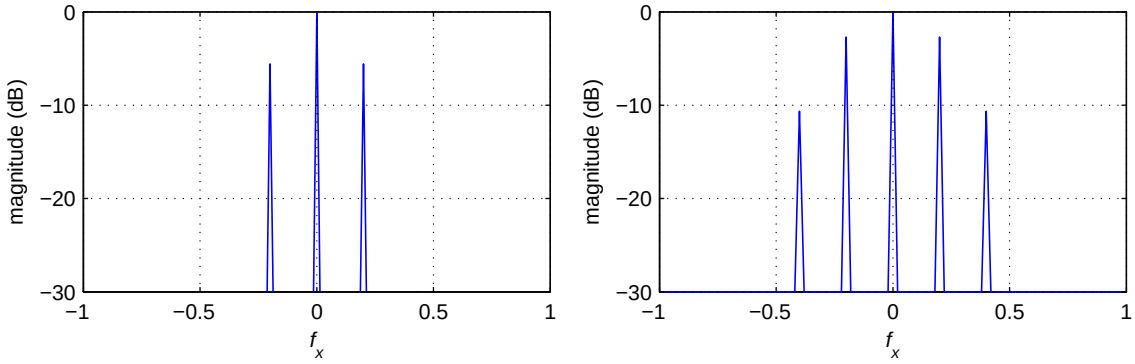

(a) (b)

Figure 14. Nonlinear distortions – Spectra along x-axis for signal (f_x, f_y) = (0.2, 0): a) Input image and b) Output image.

5.1.3 Evaluating the frequency response of the display

The third and final step in measuring the frequency response of the display consists of comparing the spectra of the above derived input and output images. In order to suppress the noise in the output image, we threshold the spectrum of each image to -30dB below the strongest frequency component. This threshold was experimentally chosen for the X3D display, but we believe that it can be used for any other display having 8bit image depth.

The criteria for determining if a given frequency component passes through the system properly or if it is distorted due to the aliasing and imaging errors was the following: for every input signal of frequency (f_{x0}, f_{y0}) we checked if the contributing aliasing / imaging components contain frequency components that are inside a circle with radius

$$r_0 = \sqrt{f_{x0}^2 + f_{y0}^2}\,, \tag{3}$$

that is, if there are signals with a lower frequency than the one used at the input. In all cases we ignored the DC component. The motivation behind this criterion is twofold. First, according to the sampling theory, aliasing will occur once the input signal is greater than half of the sampling frequency. The frequency of the aliased component is lower than the frequency of the signal itself. Therefore, the above criteria effectively checks whether aliasing occurred or not. The second motivation lies in the fact that low frequency errors (like the ones caused by aliasing) are much more visually annoying when occurring on the screen than high frequency ones (e.g. imaging). Consequently, we define the passband of the display as the region of all test frequencies which cause no additional frequency components inside radius r_0, and define the stopband everywhere else.

As an example, the magnified versions of Figure 13a and Figure 13b are shown in Figure 15a and Figure 15b, respectively. In these figures, only the part containing frequencies smaller than r_0 (represented by the circle) is shown. As seen from the figures, in the first example there are no spectral components that are of a lower frequency than the one used for generating the input image, and therefore the signal of this frequency would be in the passband. In the second example, the output image considerably differs from the one sent to the display due to the aliasing errors. In the spectral domain this can be noticed by the presence of several frequency components that are inside the circle with

radius r_0. There is no point in trying to represent images containing such input frequencies on the display under consideration.

By applying the above criteria to all the used input/output images, the passband and stopband of the display are classified as given in Figure 16a. In this figure, the passband is represented by dots. Due to measurement errors, the passband region is not continuous. It can be easily smoothened by applying a 5 by 5 median filter. The final frequency response for the X3D display is shown in Figure 16b. As expected, the frequency response of the display given in Figure 16b shows that the display is able to represent signals containing low frequencies. By following our methodology, one can obtain the passband region for an arbitrary display. This response can be used for deriving anti-aliasing filters to be applied to images before visualizing them on the display. Applying such filters will remove moiré artifacts and make masking artifacts less visible. An approach for designing efficient anti-aliasing filters for multiview displays is discussed in [14].

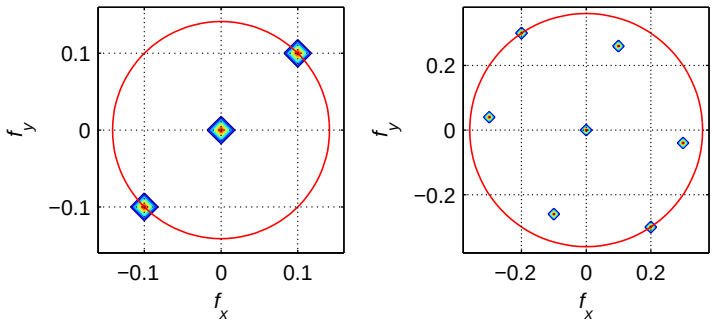

(a) (b)

Figure 15. Spectra of output images: a) (f_{x0}, f_{y0}) = (0.1, 0.1), r_0=0.14 and b) (f_{x0}, f_{y0}) = (0.2, – 0.3), r_0=0.36

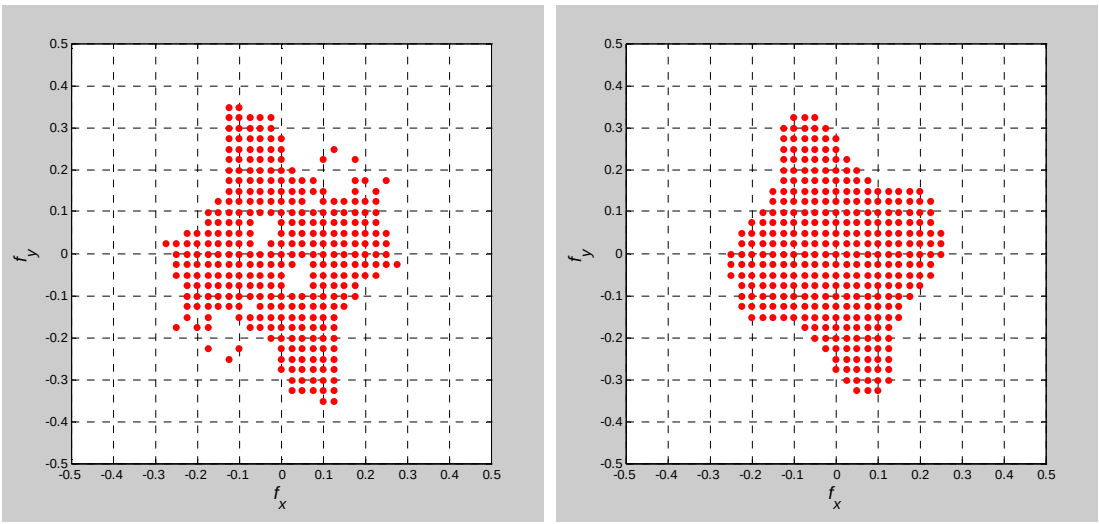

(a) (b)

Figure 16. Frequency response of the display: a) Passband region estimation based on measurements and b) Passband region after filtering.

6. CONCLUSIONS

In order to understand the reasons for artifacts in multiview display, we modeled the effect of optical layer on the underlying TFT-LCD image. Based on this model, we explained the reasons for some common artifacts. We identified which visual properties of a multiview display are needed to design image processing algorithms for artifact mitigation – namely interleaving pattern, angular visibility of sub-pixels and display performance in frequency domain.

We described a methodology for measuring and modeling these parameters, which does not require precisely positioned laboratory equipment. The methodology is simple, yet effective, and allows the end user to derive the number of images needed, the algorithm for interleaving them, and the pre-filter which would optimize the visual quality of these images for a given multiview display.

To exemplify our methodology, we presented measurement results for one multiview display. The precision of the model that we derived from the measurements is sufficient for it to be used in visual optimization algorithms[14,19].

REFERENCES

1 S. Pastoor, "3D displays", in (Schreer, Kauff, Sikora, edts.) *3D Video Communication*, Wiley, 2005.

2 J.-Y. Son and B. Javidi, "Three-Dimensional Imaging Methods Based on Multiview Images," J. Display Technol. 1, pp. 125- (2005)

3 J.-Y. Son, B. Javidi, S. Yano, K.-H. Choi, "Recent developments in 3-D imaging Technologies", J. Display Technol. 99, pp. 1-10 (2010)

4 N. Dodgson, "Autostereoscopic 3D Displays," Computer , vol.38, no.8, pp. 31- 36, Aug. 2005, IEEE (2005)

5 M. Salmimaa, T. Jarvenpaa, "Optical characterization of autostereoscopic 3-D displays", *J. Soc. Inf. Display 16*, 825 (2008)

6 C. Moller, A. Travis, Correcting Interperspective Aliasing in Autostereoscopic Displays. *IEEE Transactions on Visualization and Computer Graphics* 11, 2 (Mar. 2005), 228-236.

7 A. Schmidt and A. Grasnick, "Multi-viewpoint autostereoscopic displays from 4D-vision", *in Proc. SPIE Photonics West 2002: Electronic Imaging*, vol. 4660, pp. 212-221, 2002.

8 V. Berkel and J. Clarke, "Characterisation and optimisation of 3D-LCD module design", *in Proc. SPIE Vol. 2653, Stereoscopic Displays and Virtual Reality Systems IV*, (Fisher, Merritt, Bolas, edts.), p. 179-186, May 1997

9 J. Konrad and P. Agniel**,** "Subsampling models and anti-alias filters for 3-D automultiscopic displays," *IEEE Trans. Image Process.*, vol. 15, pp. 128-140, Jan. 2006

10 M. Salmimaa, T. Jarvenpaa, "3-D crosstalk and luminance uniformity from angular luminance profiles of multiview autostereoscopic 3-D displays", *J. Soc. Inf. Display 16*, 1033 (2008)

11 V. Saveljev, J.-Y. Son, B. Javidi, S.-K. Kim, and D.-S. Kim, "Moiré Minimization Condition in Three-Dimensional Image Displays," J. Display Technol. 1, 347- (2005)

12 J. Hakkinen, J. Takatalo, M. Kilpelainen, M. Salmimaa, and G. Nyman, "Determining limits to avoid double vision in an autostereoscopic display: Disparity and image element width", J. Soc. Inf. Display 17, 433 (2009)

13 Zwicker, M., Matusik, W., Durand, F., Pfister, H., and Forlines, C. 2006. Antialiasing for automultiscopic 3D displays. In *ACM SIGGRAPH 2006 Sketches* (Boston, Massachusetts, July 30 - August 03, 2006). SIGGRAPH '06. ACM, New York, NY, 107.

14 A. Boev, R. Bregovic, A. Gotchev, K. Egiazarian, Anti-aliasing filtering of 2D images for multi-view auto-stereoscopic displays, in Proc. of *The 2009 International Workshop on Local and Non-Local Approximation in Image Processing, LNLA 2009*, Helsinki, Finland, 2009

15 M. Becker, "Display reflectance: Basics, measurement, and rating", J. Soc. Inf. Display 14, 1003 (2006)

16 G. Woodgate, J. Harrold, "Efficiency analysis for multi-view spatially multiplexed autostereoscopic 2-D/3-D displays", J. Soc. Inf. Display 15, 873 (2007)

17 W. Mphepö, Yi-Pai Huang, and Han-Ping Shieh, "Enhancing the Brightness of Parallax Barrier Based 3D Flat Panel Mobile Displays Without Compromising Power Consumption", Journal of Display Technology, Vol. 6, Issue 2, pp. 60-64 (2010)

18 M. Krijn, S. de Zwart, D. de Boer, O. Willemsen, and M. Sluijter, "2-D/3-D displays based on switchable lenticulars", J. Soc. Inf. Display 16, 847 (2008)

19 A. Boev, K. Raunio, A. Gotchev and K. Egiazarian, "GPU-based algorithms for optimized visualization and crosstalk mitigation on a multiview display", Proc. SPIE-IS&T Electronic Imaging 2008, Stereoscopic Displays and Applications XIX, Vol. 6803, San Jose, USA, January 2008

20 P. Boher, T. Leroux, T. Bignon, V. Collomb-Patton, "A new way to characterize auto-stereoscopic 3D displays using Fourier optics instrument", in *Proc. of SPIE, Stereoscopic displays and applications XX* , 19-21 January 2008, San Jose, California, USA

21 R. Hartley, A. Zisserman, "Multiple View Geometry in Computer Vision", 2nd edition, ISBN: 0521540518, Cambridge University Press, March 2006.

22 P. Debevec, J. Malik, "Recovering High Dynamic Range Radiance Maps from Photographs," in *Proc. ACM SIGGRAPH, 1997*